J|A|C|S
ARTICLES
Published on Web 12/30/2003

New 1*H*-Pyrazole-Containing Polyamine Receptors Able To Complex L-Glutamate in Water at Physiological pH Values

Carlos Miranda,[†] Francisco Escartí,[‡] Laurent Lamarque,[†] María J. R. Yunta,[§] Pilar Navarro,*[,†] Enrique García-España,*[,‡] and M. Luisa Jimeno[†]

Contribution from the Instituto de Química Médica, Centro de Química Orgánica Manuel Lora Tamayo, CSIC, C/ Juan de la Cierva 3, 28006 Madrid, Spain, Departamento de Química Inorgánica, Facultad de Química, Universidad de Valencia, c/ Doctor Moliner 50, 46100 Burjassot (Valencia), Spain, and Departamento de Química Orgánica, Facultad de Química, Universidad Complutense de Madrid, Avda. Complutense s/n, 28040 Madrid, Spain

Received April 16, 2003; E-mail: enrique.garcia-es@uv.es

Abstract: The interaction of the pyrazole-containing macrocyclic receptors 3,6,9,12,13,16,19,22,25,26-decaazatricyclo-[22.2.1.1^{11,14}]-octacosa-1(27),11,14(28),24-tetraene **1**[$\mathbf{L_1}$], 13,26-dibenzyl-3,6,9,12,13,16,-19,22,25,26-decaazatricyclo-[22.2.1.1^{11,14}]-octacosa-1(27),11,14(28),24-tetraene **2**[$\mathbf{L_2}$], 3,9,12,13,16,22,-25,26-octaazatricyclo-[22.2.1.1^{11,14}]-octacosa-1(27),11,14(28),24-tetraene **3**[$\mathbf{L_3}$], 6,19-dibenzyl-3,6,9,12,13,-16,19,22,25,26-decaazatricyclo-[22.2.1.1^{11,14}]-octacosa-1(27),11,14(28),24-tetraene **4**[$\mathbf{L_4}$], 6,19-diphenethyl-3,6,9,12,13,16,19,22,25,26-decaazatricyclo-[22.2.1.1^{11,14}]-octacosa-1(27),11,14(28),24-tetraene **5**[$\mathbf{L_5}$], and 6,19-dioctyl-3,6,9,12,13,16,19,22,25,26-decaazatricyclo-[22.2.1.1^{11,14}]-octacosa-1(27),11,14(28),24-tetraene **6**[$\mathbf{L_6}$] with L-glutamate in aqueous solution has been studied by potentiometric techniques. The synthesis of receptors **3**−**6**[$\mathbf{L_3}$−$\mathbf{L_6}$] is described for the first time. The potentiometric results show that **4**[$\mathbf{L_4}$] containing benzyl groups in the central nitrogens of the polyamine side chains is the receptor displaying the larger interaction at pH 7.4 ($K_{\text{eff}} = 2.04 \times 10^4$). The presence of phenethyl **5**[$\mathbf{L_5}$] or octyl groups **6**[$\mathbf{L_6}$] instead of benzyl groups **4**[$\mathbf{L_4}$] in the central nitrogens of the chains produces a drastic decrease in the stability [$K_{\text{eff}} = 3.51 \times 10^2$ (**5**), $K_{\text{eff}} = 3.64 \times 10^2$ (**6**)]. The studies show the relevance of the central polyaminic nitrogen in the interaction with glutamate. **1**[$\mathbf{L_1}$] and **2**[$\mathbf{L_2}$] with secondary nitrogens in this position present significantly larger interactions than **3**[$\mathbf{L_3}$], which lacks an amino group in the center of the chains. The NMR and modeling studies suggest the important contribution of hydrogen bonding and π-cation interaction to adduct formation.

Introduction

The search for the L-glutamate receptor field has been and continues to be in a state of almost explosive development.[1] L-Glutamate (Glu) is thought to be the predominant excitatory transmitter in the central nervous system (CNS) acting at a range of excitatory amino acid receptors. It is well-known that it plays a vital role mediating a great part of the synaptic transmission.[2] However, there is an increasing amount of experimental evidence that metabolic defects and glutamatergic abnormalities can exacerbate or induce glutamate-mediated excitotoxic damage and consequently neurological disorders.[3,4] Overactivation of ionotropic (NMDA, AMPA, and Kainate) receptors (iGluRs) by Glu yields an excessive Ca^{2+} influx that produces irreversible loss of neurons of specific areas of the brain.[5] There is much evidence that these processes induce, at least in part, neurodegenerative illnesses such as Parkinson, Alzheimer, Huntington, AIDS, dementia, and amyotrophic lateral sclerosis (ALS).[6] In particular, ALS is one of the neurodegenerative disorders for which there is more evidence that excitotoxicity due to an increase in Glu concentration may contribute to the pathology of the disease.[7] Memantine, a drug able to antagonize the pathological effects of sustained, but relatively small, increases in extracellular glutamate concentration, has been recently received for the treatment of Alzheimer disease.[8] However, there is not an effective treatment for ALS. Therefore, the preparation of adequately functionalized synthetic receptors for L-glutamate seems to be an important target in finding new routes for controlling abnormal excitatory processes. However, effective recognition in water of aminocarboxylic acids is not an easy task due to its zwitterionic character at physiological pH values and to the strong competition that it finds in its own solvent.[9]

[†] Centro de Química Orgánica Manuel Lora Tamayo.
[‡] Universidad de Valencia.
[§] Universidad Complutense de Madrid.

(1) Jane, D. E. In *Medicinal Chemistry into the Millenium*; Campbell, M. M., Blagbrough, I. S., Eds.; Royal Society of Chemistry: Cambridge, 2001; pp 67−84.
(2) (a) Standaert, D. G.; Young, A. B. In *The Pharmacological Basis of Therapeutics*; Hardman, J. G., Goodman Gilman, A., Limbird, L. E., Eds.; McGraw-Hill: New York, 1996; Chapter 22, p 503. (b) Fletcher, E. J.; Loge, D. In *An Introduction to Neurotransmission in Health and Disease*; Riederer, P., Kopp, N., Pearson, J., Eds.; Oxford University Press: New York, 1990; Chapter 7, p 79.
(3) Michaelis, E. K. *Prog. Neurobiol.* **1998**, *54*, 369−415.
(4) Olney, J. W. *Science* **1969**, *164*, 719−721.
(5) Green, J. G.; Greenamyre, J. T. *Prog. Neurobiol.* **1996**, *48*, 613−63.
(6) Bräun-Osborne, H.; Egebjerg, J.; Nielsen, E. O.; Madsen, U.; Krogsgaard-Larsen, P. *J. Med. Chem.* **2000**, *43*, 2609−2645 and references therein.
(7) (a) Shaw, P. J.; Ince, P. G. *J. Neurol.* **1997**, *244* (Suppl 2), S3−S14. (b) Plaitakis, A.; Fesdjian, C. O.; Shashidharan, P. *CNS Drugs* **1996**, *5*, 437−456.
(8) Frantz, A.; Smith, A. *Nat. Rev. Drug Dicovery* **2003**, *2*, 9.

Chart 1. Some Receptors Employed for Dicarboxylic Acid and *N*-Acetylglutamate Recognition

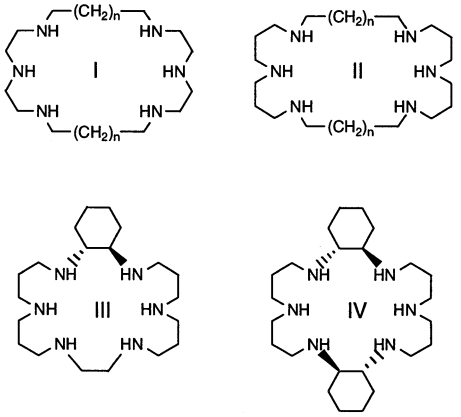

There are many types of receptors able to interact with carboxylic acids and amino acids in organic solvents,[10−13] yielding selective complexation in some instances. However, the number of reported receptors of glutamate in aqueous solution is very scarce. In this sense, one of the few reports concerns an optical sensor based on a Zn(II) complex of a 2,2′:6′,2″-terpyridine derivative in which L-aspartate and L-glutamate were efficiently bound as axial ligands ($K_s = 10^4-10^5\ M^{-1}$) in 50/50 water/methanol mixtures.[14]

Among the receptors employed for carboxylic acid recognition, the polyamine macrocycles **I**−**IV** in Chart 1 are of particular relevance to this work. In a seminal paper, Lehn et al.[15] showed that saturated polyamines **I** and **II** could exert chain-length discrimination between different α,ω-dicarboxylic acids as a function of the number of methylene groups between the two triamine units of the receptor. Such compounds were also able to interact with a glutamic acid derivative which has the ammonium group protected with an acyl moiety.[15,16] Compounds **III** and **IV** reported by Gotor and Lehn interact in their protonated forms in aqueous solution with protected *N*-acetyl-L-glutamate and *N*-acetyl-D-glutamate, showing a higher stability for the interaction with the D-isomer.[17] In both reports, the interaction with protected *N*-acetyl-L-glutamate at physiological pH yields constants of ca. 3 logarithmic units.

Recently, we have shown that 1*H*-pyrazole-containing macrocycles present desirable properties for the binding of dopamine.[18] These polyaza macrocycles, apart from having a high positive charge at neutral pH values, can form hydrogen bonds not only through the ammonium or amine groups but also through the pyrazole nitrogens that can behave as hydrogen bond donors or acceptors. In fact, Elguero et al.[19] have recently shown the ability of the pyrazole rings to form hydrogen bonds with carboxylic and carboxylate functions. These features can be used to recognize the functionalities of glutamic acid, the carboxylic and/or carboxylate functions and the ammonium group.

Chart 2. New 1*H*-Pyrazole-Containing Polyamine Receptors Able To Complex L-Glutamate in Water

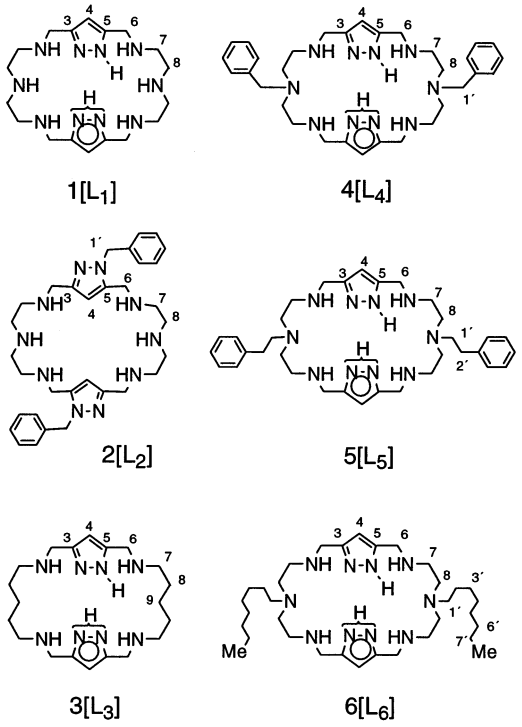

Apart from this, the introduction of aromatic donor groups appropriately arranged within the macrocyclic framework or appended to it through arms of adequate length may contribute to the recognition event through π-cation interactions with the ammonium group of L-glutamate. π-Cation interactions are a key feature in many enzymatic centers, a classical example being acetylcholine esterase.[20] The role of such an interaction in abiotic systems was very well illustrated several years ago in a seminal work carried out by Dougherty and Stauffer.[21] Since then, many other examples have been reported both in biotic and in abiotic systems.[22]

Taking into account all of these considerations, here we report on the ability of receptors **1**[**L**$_1$]−**6**[**L**$_6$] (Chart 2) to interact with L-glutamic acid. These receptors display structures which differ from one another in only one feature, which helps to obtain clear-cut relations between structure and interaction

(9) Rebek, J., Jr.; Askew, B.; Nemeth, D.; Parris, K. *J. Am. Chem. Soc.* **1987**, *109*, 2432−2434.
(10) Seel, C.; de Mendoza, J. In *Comprehensive Supramolecular Chemistry*; Vogtle, F., Ed.; Elsevier Science: New York, 1996; Vol. 2, p 519.
(11) (a) Sessler, J. L.; Sanson, P. I.; Andrievesky, A.; Kral, V. In *Supramolecular Chemistry of Anions*; Bianchi, A., Bowman-James, K., García-España, E., Eds.; John Wiley & Sons: New York, 1997; Chapter 10, pp 369−375. (b) Sessler, J. L.; Andrievsky, A.; Král, V.; Lynch, V. *J. Am. Chem. Soc.* **1997**, *119*, 9385−9392.
(12) Fitzmaurice, R. J.; Kyne, G. M.; Douheret, D.; Kilburn, J. D. *J. Chem. Soc., Perkin Trans. 1* **2002**, *7*, 841−864 and references therein.
(13) Rossi, S.; Kyne, G. M.; Turner, D. L.; Wells, N. J.; Kilburn, J. D. *Angew. Chem., Int. Ed.* **2002**, *41*, 4233−4236.
(14) Aït-Haddou, H.; Wiskur, S. L.; Lynch, V. M.; Anslyn, E. V. *J. Am. Chem. Soc.* **2001**, *123*, 11296−11297.
(15) Hosseini, M. W.; Lehn, J.-M. *J. Am. Chem. Soc.* **1982**, *104*, 3525−3527.
(16) (a) Hosseini, M. W.; Lehn, J.-M. *Helv. Chim. Acta* **1986**, *69*, 587−603. (b) Heyer, D.; Lehn, J.-M. *Tetrahedron Lett.* **1986**, *27*, 5869−5872.
(17) (a) Alfonso, I.; Dietrich, B.; Rebolledo, F.; Gotor, V.; Lehn, J.-M. *Helv. Chim. Acta* **2001**, *84*, 280−295. (b) Alfonso, I.; Rebolledo, F.; Gotor, V. *Chem.-Eur. J.* **2000**, *6*, 3331−3338.
(18) Lamarque, L.; Navarro, P.; Miranda, C.; Arán, V. J.; Ochoa, C.; Escartí, F.; García-España, E.; Latorre, J.; Luis, S. V.; Miravet, J. F. *J. Am. Chem. Soc.* **2001**, *123*, 10560−10570.
(19) Foces-Foces, C.; Echevarria, A.; Jagerovic, N.; Alkorta, I.; Elguero, J.; Langer, U.; Klein, O.; Minguet-Bonvehí, H.-H. *J. Am. Chem. Soc.* **2001**, *123*, 7898−7906.
(20) Sussman, J. L.; Harel, M.; Frolow, F.; Oefner, C.; Goldman, A.; Toker, L.; Silman, I. *Science* **1991**, *253*, 872−879.
(21) Dougherty, D. A.; Stauffer, D. A. *Science* **1990**, *250*, 1558−1560.
(22) (a) Sutcliffe, M. J.; Smeeton, A. H.; Wo, Z. G.; Oswald, R. E. *Faraday Discuss.* **1998**, *111*, 259−272. (b) Kearney, P. C.; Mizoue, L. S.; Kumpf, R. A.; Forman, J. E.; McCurdy, A.; Dougherty, D. A. *J. Am. Chem. Soc.* **1993**, *115*, 9907−9919. (c) Bräuner-Osborne, H.; Egebjerg, J.; Nielsen, E.; Madsen, U.; Krogsgaard-Larsen, P. *J. Med. Chem.* **2000**, *43*, 2609−2645. (d) Zacharias, N.; Dougherty, D. A. *Trends Pharmacol. Sci.* **2002**, *23*, 281−287. (e) Hu, J.; Barbour, L. J.; Gokel, G. W. *J. Am. Chem. Soc.* **2002**, *124*, 10940−10941.

strengths. **1**[$\mathbf{L_1}$] and **2**[$\mathbf{L_2}$] differ in the *N*-benzylation of the pyrazole moiety, and **1**[$\mathbf{L_1}$] and **3**[$\mathbf{L_3}$] differ in the presence in the center of the polyamine side chains of an amino group or of a methylene group. The receptors **4**[$\mathbf{L_4}$] and **5**[$\mathbf{L_5}$] present the central nitrogens of the chain *N*-functionalized with benzyl or phenethyl groups, and **6**[$\mathbf{L_6}$] has large hydrophobic octyl groups.

Results and Discussion

Synthesis of 3−6. Macrocycles **3**−**6** have been obtained following the procedure previously reported for the preparation of **1** and **2**.[23] The method includes a first dipodal (2+2) condensation of the 1*H*-pyrazol-3,5-dicarbaldehyde **7** with the corresponding α,ω-diamine, followed by hydrogenation of the resulting Schiff base imine bonds. In the case of receptor **3**, the Schiff base formed by condensation with 1,5-pentanediamine is a stable solid (**8**, mp 208−210 °C) which precipitated in 68% yield from the reaction mixture. Further reduction with $NaBH_4$ in absolute ethanol gave the expected tetraazamacrocycle **3**, which after crystallization from toluene was isolated as a pure compound (mp 184−186 °C). In the cases of receptors **4**−**6**, the precursor α,ω-diamines (**11a**−**11c**) (Scheme 1B) were obtained, by using a procedure previously described for **11a**.[24] This procedure is based on the previous protection of the primary amino groups of 1,5-diamino-3-azapentane by treatment with phthalic anhydride, followed by alkylation of the secondary amino group of 1,5-diphthalimido-3-azapentane **9** with benzyl, phenethyl, or octyl bromide. Finally, the phthalimido groups of the *N*-alkyl substituted intermediates **10a**−**10c** were removed by treatment with hydrazine to afford the desired amines **11a**−**11c**, which were obtained in moderate yield (54−63%).

In contrast with the behavior previously observed in the synthesis of **3**, in the (2+2) dipodal condensations of **7** with 3-benzyl-, 3-phenethyl-, and 3-octyl-substituted 3-aza-1,5-pentanediamine **11a**, **11b**, and **11c**, respectively, there was not precipitation of the expected Schiff bases (Scheme 1A). Consequently, the reaction mixtures were directly reduced in situ with $NaBH_4$ to obtain the desired hexaamines **4**−**6**, which after being carefully purified by chromatography afforded pure colorless oils in 51%, 63%, and 31% yield, respectively. The structures of all of these new cyclic polyamines have been established from the analytical and spectroscopic data (MS(ES^+), ^1H and ^{13}C NMR) of both the free ligands **3**−**6** and their corresponding hydrochloride salts [**3**·4HCl, **4**·6HCl, **5**·6HCl, and **6**·6HCl], which were obtained as stable solids following the same procedure previously reported[18] for **1**·6HCl and **2**·6HCl.

As usually occurs for 3,5-disubstituted 1*H*-pyrazole derivatives, either the free ligands **3**−**6** or their hydrochlorides show very simple ^1H and ^{13}C NMR spectra, in which signals indicate that, because of the prototropic equilibrium of the pyrazole ring, all of these compounds present average 4-fold symmetry on the NMR scale. The quaternary C_3 and C_5 carbons appear together, and the pairs of methylene carbons C_6, C_7, and C_8 are magnetically equivalent (see Experimental Section).

In the ^{13}C NMR spectra registered in $CDCl_3$ solution, significant differences can be observed between ligand **3**, without an amino group in the center of the side chain, and the *N*-substituted ligands **4**−**6**. In **3**, the $C_{3,5}$ signal appears as a broad singlet. However, in **4**−**6**, it almost disappears within the baseline of the spectra, and the methylene carbon atoms C_6 and C_8 experience a significant broadening. Additionally, a remarkable line-broadening is also observed in the C_1' carbon signals belonging to the phenethyl and octyl groups of $\mathbf{L_5}$ and $\mathbf{L_6}$, respectively. All of these data suggest that as the *N*-substituents located in the middle of the side chains of **4**−**6** are larger, the dynamic exchange rate of the pyrazole prototropic equilibrium is gradually lower, probably due to a relation between prototropic and conformational equilibria.

Scheme 1. Synthesis of the Pyrazole-Containing Macrocyclic Receptors

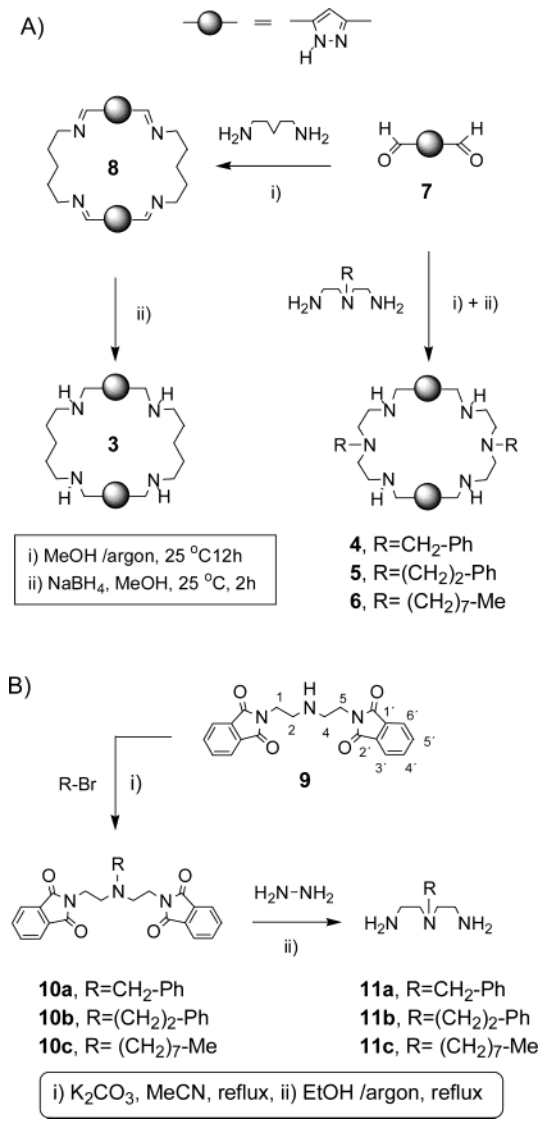

Acid−Base Behavior. To follow the complexation of L-glutamate (hereafter abbreviated as Glu^{2-}) and its protonated forms ($HGlu^-$, H_2Glu, and H_3Glu^+) by the receptors $\mathbf{L_1}$−$\mathbf{L_6}$, the acid−base behavior of L-glutamate has to be revisited under the experimental conditions of this work, 298 K and 0.15 mol dm^{-3}. The protonation constants obtained, included in the first column of Table 1, agree with the literature[25] and show that the zwitterionic $HGlu^-$ species is the only species present in aqueous solution at physiological pH values (Scheme 2 and Figure S_1 of Supporting Information). Therefore, receptors for

(23) Arán, V. J.; Kumar, M.; Molina, J.; Lamarque, L.; Navarro, P.; García-España, E.; Ramírez, J. A.; Luis, S. V.; Escuder, B. *J. Org. Chem.* **1999**, *64*, 6137−6146.

(24) (a) Yuen Ng, C.; Motekaitis, R. J.; Martell, A. E. *Inorg. Chem.* **1979**, *18*, 2982−2986. (b) Anelli, P. L.; Lunazzi, L.; Montanari, F.; Quici, S. *J. Org. Chem.* **1984**, *49*, 4197−4203.

Table 1. Protonation Constants of Glutamic Acid and Receptors $\mathbf{L_1}-\mathbf{L_6}$ Determined in NaCl 0.15 mol dm^{-3} at 298.1 K

reaction	Glu	L_1[a]	L_2[a]	L_3[b]	L_4	L_5	L_6
$L + H = LH$[c]	9.574 (2)[d]	9.74 (2)	8.90 (3)	9.56 (1)	9.25 (3)	9.49 (4)	9.34 (5)
$LH + H = LH_2$	4.165 (3)	8.86 (2)	8.27 (2)	8.939 (7)	8.38 (3)	8.11 (5)	8.13 (5)
$LH_2 + H = LH_3$	2.18 (2)	7.96 (2)	6.62 (3)	8.02 (1)	6.89 (5)	7.17 (6)	7.46 (7)
$LH_3 + H = LH_4$		6.83 (2)	5.85 (4)	7.63 (1)	6.32 (5)	6.35 (6)	5.97 (8)
$LH_4 + H = LH_5$		4.57 (3)	3.37 (4)		2.72 (8)	2.84 (9)	3.23 (9)
$LH_5 + H = LH_6$		3.18 (3)	2.27 (6)				
$\sum \log K_{H_nL}$		41.1	35.3	34.2	33.6	34.0	34.1

[a] Taken from ref 23. [b] These data were previously cited in a short communication (ref 26). [c] Charges omitted for clarity. [d] Values in parentheses are the standard deviations in the last significant figure.

Scheme 2. L-Glutamate Acid−Base Behavior

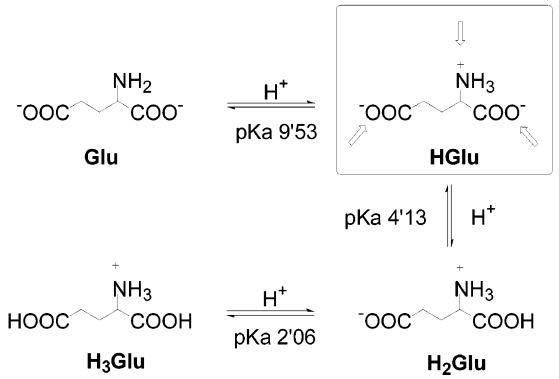

glutamate recognition able to address both the negative charges of the carboxylate groups and the positive charge of ammonium are highly relevant.

The protonation constants of $\mathbf{L_3}-\mathbf{L_6}$ are included in Table 1, together with those we have previously reported for receptors $\mathbf{L_1}$ and $\mathbf{L_2}$.[23] A comparison of the constants of $\mathbf{L_4}-\mathbf{L_6}$ with those of the nonfunctionalized receptor $\mathbf{L_1}$ shows a reduced basicity of the receptors $\mathbf{L_4}-\mathbf{L_6}$ with tertiary nitrogens at the middle of the polyamine bridges. Such a reduction in basicity prevented the potentiometric detection of the last protonation for these ligands in aqueous solution. A similar reduction in basicity was previously reported for the macrocycle with the *N*-benzylated pyrazole spacers ($\mathbf{L_2}$).[23] These diminished basicities are related to the lower probability of the tertiary nitrogens for stabilizing the positive charges through hydrogen bond formation either with adjacent nonprotonated amino groups of the molecule or with water molecules. Also, the increase in the hydrophobicity of these molecules will contribute to their lower basicity. The stepwise basicity constants are relatively high for the first four protonation steps, which is attributable to the fact that these protons can bind to the nitrogen atoms adjacent to the pyrazole groups leaving the central nitrogen free, the electrostatic repulsions between them being therefore of little significance. The remaining protonation steps will occur in the central nitrogen atom, which will produce an important increase in the electrostatic repulsion in the molecule and therefore a reduction in basicity. As stated above, the tertiary nitrogen atoms present in $\mathbf{L_4}-\mathbf{L_6}$ will also contribute to this diminished basicity.

To analyze the interaction with glutamic acid, it is important to know the protonation degree of the ligands at physiological pH values. In Table 2, we have calculated the percentages of the different protonated species existing in solution at pH 7.4 for receptors $\mathbf{L_1}-\mathbf{L_6}$. As can be seen, except for the receptor with the pentamethylenic chains $\mathbf{L_3}$ in which the tetraprotonated species prevails, all of the other systems show that the di- and triprotonated species prevail, although to different extents.

Table 2. Percentages of the Different Protonated Species at pH 7.4

	H_1L[a]	H_2L	H_3L	H_4L
$\mathbf{L_1}$	1	18	**64**	17
$\mathbf{L_2}$	10	**77**	13	0
$\mathbf{L_3}$	0	8	34	**58**
$\mathbf{L_4}$	0	8	34	**58**
$\mathbf{L_5}$	11	**54**	32	3
$\mathbf{L_6}$	8	42	**48**	2

[a] Charges omitted for clarity.

Interaction with Glutamate. The stepwise constants for the interaction of the receptors $\mathbf{L_1}-\mathbf{L_6}$ with glutamate are shown in Table 3, and selected distribution diagrams are plotted in Figure 1A−C.

All of the studied receptors interact with glutamate forming adduct species with protonation degrees (j) which vary between 8 and 0 depending on the system (see Table 3). The stepwise constants have been derived from the overall association constants ($L + Glu^{2-} + jH^+ = H_jLGlu^{(j-2)+}$, $\log \beta_j$) provided by the fitting of the pH-metric titration curves. This takes into account the basicities of the receptors and glutamate (vide supra) and the pH range in which a given species prevails in solution. In this respect, except below pH ca. 4 and above pH 9, $HGlu^-$ can be chosen as the protonated form of glutamate involved in the formation of the different adducts. Below pH 4, the participation of H_2Glu in the equilibria has also to be considered (entries 9 and 10 in Table 3). For instance, the formation of the H_6LGlu^{4+} species can proceed through the equilibria $HGlu^- + H_5L^{5+} = H_6LGlu^{4+}$ (entry 8, Table 3), and $H_2Glu + H_4L^{4+} = H_6LGlu^4$ (entry 9 Table 3), with percentages of participation that depend on pH. One of the effects of the interaction is to render somewhat more basic the receptor, and somewhat more acidic glutamic acid, facilitating the attraction between oppositely charged partners.

A first inspection of Table 3 and of the diagrams A, B, and C in Figure 1 shows that the interaction strengths differ markedly from one system to another depending on the structural features of the receptors involved. $\mathbf{L_4}$ is the receptor that presents the highest capacity for interacting with glutamate throughout all of the pH range explored. It must also be remarked that there are not clear-cut trends in the values of the stepwise constants as a function of the protonation degree of the receptors. This suggests that charge−charge attractions do not play the most

(25) (a) Martell, E.; Smith, R. M. *Critical Stability Constants*; Plenum: New York, 1975. (b) Motekaitis, R. J. NIST *Critically Selected Stability Constants of Metal Complexes Database*; NIST Standard Reference Database, version 4, 1997.

Table 3. Stability Constants for the Interaction of $\mathbf{L_1}$−$\mathbf{L_6}$ with the Different Protonated Forms of Glutamate (Glu)

entry	reaction[a]	L_1	L_2	L_3	L_4	L_5	L_6
1	Glu + **L** = Glu**L**	3.30 (2)[b]	4.11 (1)				
2	HGlu + **L** = HGlu**L**	3.65 (2)	4.11 (1)		3.68 (2)		3.38 (4)
3	Glu + H**L** = HGlu**L**	3.89 (2)	4.48 (1)		3.96 (2)		3.57 (4)
4	HGlu + H**L** = H_2Glu**L**	3.49 (2)	3.89 (1)	2.37 (4)	3.71 (2)		
5	HGlu + H_2**L** = H_3Glu**L**	3.44 (2)	3.73 (1)	2.34 (3)	4.14 (2)	2.46 (4)	2.61 (7)
6	HGlu + H_3**L** = H_4Glu**L**	3.33 (2)	3.56 (2)	2.66 (3)	4.65 (2)	2.74 (3)	2.55 (7)
7	HGlu + H_4**L** = H_5Glu**L**	3.02 (2)	3.26 (2)	2.58 (3)	4.77 (2)	2.87 (3)	2.91 (5)
8	HGlu + H_5**L** = H_6Glu**L**	3.11 (3)	3.54 (2)		6.76 (3)	4.96 (3)	4.47 (3)
9	H_2Glu + H_4**L** = H_6Glu**L**	2.54 (3)	3.05 (2)	3.88 (2)	5.35 (3)	3.66 (4)	3.56 (3)
10	H_2Glu + H_5**L** = H_7Glu**L**	2.61 (6)	2.73 (4)		5.51 (3)	3.57 (4)	3.22 (8)
11	H_3Glu + H_4**L** = H_7Glu**L**			4.82 (2)			4.12 (9)

[a] Charges omitted for clarity. [b] Values in parentheses are standard deviations in the last significant figure.

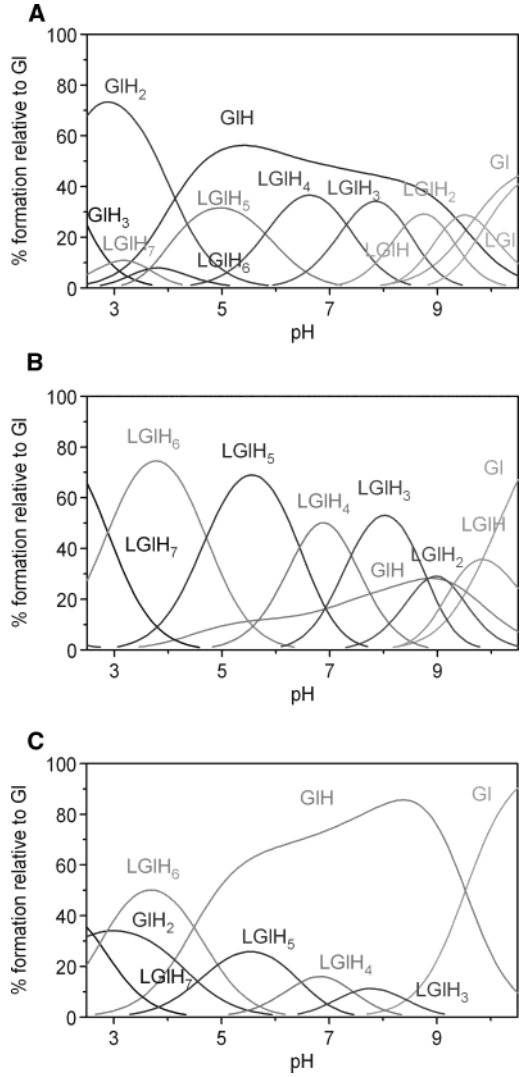

Figure 1. Distribution diagrams for the systems (A) $\mathbf{L_1}$−glutamic acid, (B) $\mathbf{L_4}$−glutamic acid, and (C) $\mathbf{L_5}$−glutamic acid.

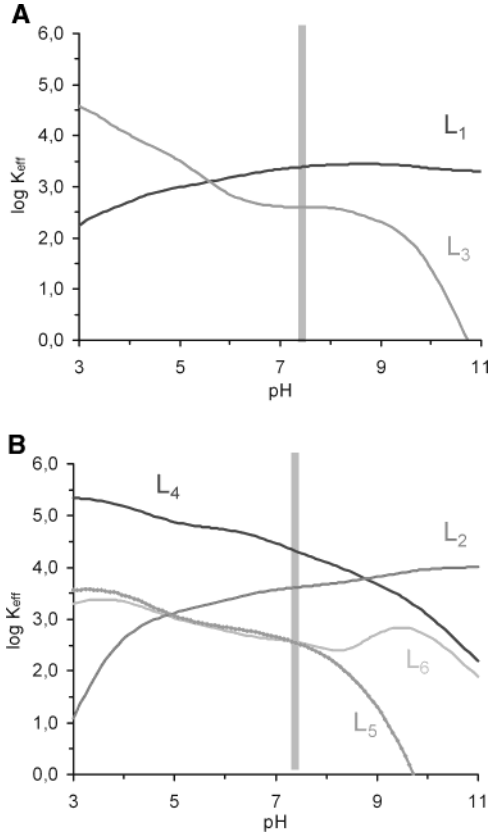

Figure 2. Representation of the variation of K_{cond} (M^{-1}) for the interaction of glutamic acid with (A) $\mathbf{L_1}$ and $\mathbf{L_3}$, (B) $\mathbf{L_2}$, $\mathbf{L_4}$, $\mathbf{L_5}$, and $\mathbf{L_6}$. Initial concentrations of glutamate and receptors are 10^{-3} mol dm^{-3}.

outstanding role and that other forces contribute very importantly to these processes.[26]

However, in systems such as these, which present overlapping equilibria, it is convenient to use conditional constants because they provide a clearer picture of the selectivity trends.[27] These constants are defined as the quotient between the overall amounts of complexed species and those of free receptor and substrate at a given pH [eq 1].

$$K_{cond} = \sum[(H_iL)\cdot(H_jGlu)]/\{\sum[H_iL]\sum[H_jGlu]\} \quad (1)$$

In Figure 2 are presented the logarithms of the effective constants versus pH for all of the studied systems. Receptors $\mathbf{L_1}$ and $\mathbf{L_2}$ with a nonfunctionalized secondary amino group in the side chains display opposite trend from all other receptors. While the stability of the $\mathbf{L_1}$ and $\mathbf{L_2}$ adducts tends to increase with pH, the other ligands show a decreasing interaction. Additionally, $\mathbf{L_1}$ and $\mathbf{L_2}$ present a close interaction over the entire pH range under study. The tetraaminic macrocycle $\mathbf{L_3}$ is a better

(26) Escartí, F.; Miranda, C.; Lamarque, L.; Latorre, J.; García-España, E.; Kumar, M.; Arán, V. J.; Navarro, P. *Chem. Commun.* **2002**, *9*, 936−937.

(27) (a) Bianchi, A.; García-España, A. *J. Chem. Educ.* **1999**, *12*, 1725−1732. (b) Aguilar, J. A.; Celda, B.; García-España, E.; Luis, S. V.; Martínez, M.; Ramírez, J. A.; Soriano, C.; Tejero, B. *J. Chem. Soc., Perkin Trans. 2* **2000**, *7*, 1323−1328.

Table 4. Percentages of the Different Protonated Adducts $[HGlu{\cdot}H_j\mathbf{L}]^{(j-1)+}$, Overall Percentages of Complexation, and Conditional Constants (K_{Cond}) at pH 7.4 for the Interaction of Glutamate ($HGlu^-$) with Receptors $\mathbf{L_1}-\mathbf{L_6}$ at Physiological pH

	$[H_nL{\cdot}HGlu]^a$					
	$n=1$	$n=2$	$n=3$	$n=4$	$\sum\{[H_nL{\cdot}HGlu]\}$	K_{cond} (M^{-1})
$\mathbf{L_1}$	3	27	23		53	2.44×10^3
$\mathbf{L_2}$	9	47	7		63	4.12×10^3
$\mathbf{L_3}$		1	10	13	24	3.99×10^2
$\mathbf{L_4}$	2	37	37	5	81	2.04×10^4
$\mathbf{L_5}$		10	10	2	22	3.51×10^2
$\mathbf{L_6}$		12	12		24	3.64×10^2

[a] Charges omitted for clarity.

receptor at acidic pH, but its interaction markedly decreases on raising the pH. These results strongly suggest the implication of the central nitrogens of the lateral polyamine chains in the stabilization of the adducts.

Among the *N*-functionalized receptors, $\mathbf{L_4}$ presents the largest interaction with glutamate. Interestingly enough, $\mathbf{L_5}$, which differs from $\mathbf{L_4}$ only in having a phenethyl group instead of a benzyl one, presents much lower stability of its adducts. Since the basicity and thereby the protonation states that $\mathbf{L_4}$ and $\mathbf{L_5}$ present with pH are very close, the reason for the larger stability of the $\mathbf{L_4}$ adducts could reside on a better spatial disposition for forming π-cation interactions with the ammonium group of the amino acid. In addition, as already pointed out, $\mathbf{L_4}$ presents the highest affinity for glutamic acid in a wide pH range, being overcome only by $\mathbf{L_1}$ and $\mathbf{L_2}$ at pH values over 9. This observation again supports the contribution of π-cation interactions in the system $\mathbf{L_4}-$glutamic because at these pH values the ammonium functionality will start to deprotonate (see Scheme 2 and Figure 1B).

Table 4 gathers the percentages of the species existing in equilibria at pH 7.4 together with the values of the conditional constant at this pH. In correspondence with Figure 1A, 1C and Figure S_2 (Supporting Information), it can be seen that for $\mathbf{L_1}$, $\mathbf{L_2}$, $\mathbf{L_5}$, and $\mathbf{L_6}$ the prevailing species are $[H_2L{\cdot}HGlu]^+$ and $[H_3L{\cdot}HGlu]^{2+}$ (protonation degrees 3 and 4, respectively), while for $\mathbf{L_3}$ the main species are $[H_3L{\cdot}HGlu]^+$ and $[H_4L{\cdot}HGlu]^{2+}$ (protonation degrees 4 and 5, respectively). The most effective receptor at this pH would be $\mathbf{L_4}$ which joins hydrogen bonding, charge−charge, and π-cation contributions for the stabilization of the adducts. To check the selectivity of this receptor, we have also studied its interaction with L-aspartate, which is a competitor of L-glutamate in the biologic receptors. The conditional constant at pH 7.4 has a value of 3.1 logarithmic units for the system Asp-$\mathbf{L_4}$. Therefore, the selectivity of $\mathbf{L_4}$ for glutamate over aspartate ($K_{cond}(\mathbf{L_4}\text{-glu})/K_{cond}(\mathbf{L_4}\text{-asp})$) will be of ca. 15. It is interesting to remark that the affinity of $\mathbf{L_4}$ for zwiterionic L-glutamate at pH 7.4 is even larger than that displayed by receptors III and IV (Chart 1) with the protected dianion *N*-acetyl-L-glutamate lacking the zwitterionic characteristics. Applying eq 1 and the stability constants reported in ref 17, conditional constants at pH 7.4 of 3.24 and 2.96 logarithmic units can be derived for the systems **III**-L-Glu and **IV**-L-Glu, respectively.

Molecular Modeling Studies. Molecular mechanics-based methods involving docking studies have been used to study the binding orientations and affinities for the complexation of glutamate by $\mathbf{L_1}-\mathbf{L_6}$ receptors.

The quality of a computer simulation depends on two factors: accuracy of the force field that describes intra- and intermolecular interactions, and an adequate sampling of the conformational and configuration space of the system.[28] The additive AMBER force field is appropriate for describing the complexation processes of our compounds, as it is one of the best methods[29] in reproducing H-bonding and stacking stabilization energies.

The experimental data show that at pH 7.4, $\mathbf{L_1}-\mathbf{L_6}$ exist in different protonation states. So, a theoretical study of the protonation of these ligands was done, including all of the species shown in 5% or more abundance in the potentiometric measurements (Table 4). In each case, the more favored positions of protons were calculated for mono-, di-, tri-, and tetraprotonated species. Molecular dynamics studies were performed to find the minimum energy conformations with simulated solvent effects.

Molecular modeling studies were carried out using the AMBER[30] method implemented in the Hyperchem 6.0 package,[31] modified by the inclusion of appropriate parameters. Where available, the parameters came from analogous ones used in the literature.[32] All others were developed following Kollman[33] and Hopfinger[34] procedures. The equilibrium bond length and angle values came from experimental values of reasonable reference compounds. All of the compounds were constructed using standard geometry and standard bond lengths. To develop suitable parameters for NH···N hydrogen bonding, ab initio calculations at the STO-3G level[35] were used to calculate atomic charges compatible with the AMBER force field charges, as they gave excellent results, and, at the same time, this method allows the study of aryl−amine interactions. In all cases, full geometry optimizations with the Polak−Ribiere algorithm were carried out, with no restraints.

Ions are separated far away and well solvated in water due to the fact that water has a high dielectric constant and hydrogen bond network. Consequently, there is no need to use counterions[36] in the modelization studies. In the absence of explicit solvent molecules, a distance-dependent dielectric factor qualitatively simulates the presence of water, as it takes into account the fact that the intermolecular electrostatic interactions should vanish more rapidly with distance than in the gas phase. The same results can be obtained using a constant dielectric factor greater than 1. We have chosen to use a distance-dependent dielectric constant ($\epsilon = 4R_{ij}$) as this was the method used by Weiner et al.[37] to develop the AMBER force field. Table 8 shows the theoretical differences in protonation energy (ΔE_p) of mono-, bi-, and triprotonated hexaamine ligands, for the

(28) Urban, J. J.; Cronin, C. W.; Roberts, R. R.; Famini, G. R. *J. Am. Chem. Soc.* **1997**, *119*, 12292−12299.
(29) Hobza, P.; Kabelac, M.; Sponer, J.; Mejzlik, P.; Vondrasek, J. *J. Comput. Chem.* **1997**, *18*, 1136−1150.
(30) Cornell, W. D.; Cieplak, P.; Bayly, C. I.; Gould, I. R.; Merz, K. M., Jr.; Ferguson, D. M.; Spelmeyer, D. C.; Fox, T.; Caldwell, J. W.; Kollman, P. A. *J. Am. Chem. Soc.* **1995**, *117*, 5179−5197.
(31) Hyperchem 6.0 (Hypercube Inc.).
(32) (a) Fox, T.; Scanlan, T. S.; Kollman, P. A. *J. Am. Chem. Soc.* **1997**, *119*, 11571−11577. (b) Grootenhuis, P. D.; Kollman, P. A. *J. Am. Chem. Soc.* **1989**, *111*, 2152−2158. (c) Moyna, G.; Hernandez, G.; Williams, H. J.; Nachman, R. J.; Scott, A. I. *J. Chem. Inf. Comput. Sci.* **1997**, *37*, 951−956. (d) Boden, C. D. J.; Patenden, G. *J. Comput.-Aided Mol. Des.* **1999**, *13*, 153−166.
(33) http://www.amber.ucsf.edu/amber.
(34) Hopfinger, A. J.; Pearlstein, R. A. *J. Comput. Chem.* **1984**, *5*, 486-499.
(35) Glennon, T. M.; Zheng, Y.-J.; Le Grand, S. M.; Shutzberg, B. A.; Merz, K. M., Jr. *J. Comput. Chem.* **1994**, *15*, 1019−1040.
(36) Wang, J.; Kollman, P. A. *J. Am. Chem. Soc.* **1998**, *120*, 11106−11114.

Table 5. Differences in Theoretical Protonation Energies (ΔE_p, kJ mol^{-1}) as a Function of Macrocyclic Nitrogen Positions and the Number of Protonated Nitrogens of Hexaamine Receptors **L_1**, **L_2**, **L_4**−**L_6**

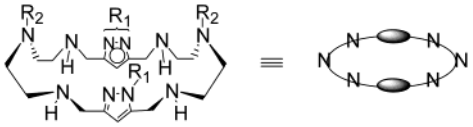

[L_n], R_1=H, Bn; R_2=H, Bn, Fen, n-Oct.

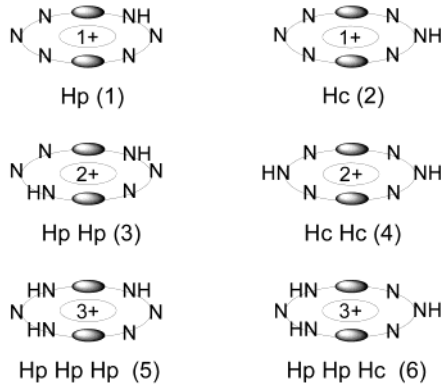

	[HL]ΔE_p (2 − 1)	[H_2L]ΔE_p (4 − 3)	[H_3L]ΔE_p (6 − 5)
L_1		−5.81	−4.35
L_2	3.18	8.44	1.38
L_4		18.40	−2.89
L_5		11.39	−8.40
L_6		20.23	−4.05

different possible positions of the protons. As can be seen, theoretical values agree with the experimental results previously obtained for **L_1** and **L_2** from a NMR study in D_2O at variable pH.[23] In **L_1**, the pattern for the protonation sequence is as follows: two protons are preferably located on the central nitrogen atoms of the macrocyclic cavity, HcHc (4), while the more stable triprotonated species correspond to a HpHpHc (6) disposition, with two protons located on nitrogen atoms adjacent to the pyrazole ring of one chain and the third one in the middle of the opposite chain (see scheme of Table 5).

On the other hand, in **L_2** the theoretical protonation energies favor the following dispositions: Hp for monoprotonated compounds (1), HpHp for the diprotonated ones (3), and HpHpHp for the triprotonated species (5), with all successive protons on adjacent positions to the pyrazole nitrogen. Finally, in **L_4**−**L_6**, the protonation sequence is as follows: two protons prefer to locate on adjacent positions to the pyrazole nitrogen HpHp (3), while the more stable triprotonated species correspond to a HpHpHc (6). Nevertheless, theoretical energy differences for HpHpHp (5) and HpHpHc (6) species are small enough [ΔE_p (6 − 5) = 8.5 kJ mol^{-1}] to consider both possibilities in the interaction with glutamate. Lowest energy conformers for all protonation states showing more than 5% abundance in potentiometric assays were located by performing simulated annealing at 400 K. These conformers were used for docking.

The energy of complexation was calculated for each compound after minimization of the selected trajectory frames, as the difference between the energy of the complex and individual energies of the glutamate and ligand.

$$E_{\text{complexation}} = E_{\text{complex}} - (E_{\text{glutamate}} + E_{\text{ligand}}) \qquad (2)$$

Table 6 shows the calculated values of complexation energies for each species (ΔE_{Cn}, kJ mol^{-1}, where n is the protonation state), the contribution to the total energy as a function of their relative abundance (%ΔE_{Cn}, kJ mol^{-1}), and total energy for complexation of each receptor with glutamate (ΔE_{TC}) as the sum of all of these partial contributions $\sum$[(%ΔE_{Cn}], together with experimental values of effective association stability constants (K_{eff}, M^{-1}). Relative values of ΔE_{TC} show that our modeling calculations are in excellent agreement with experimental K_{eff} data obtained for **L_1**−**L_6** as they exhibit the same trend: **L_4** ≫ **L_2** > **L_1** ≫ **L_3** > **L_6** > **L_5**.

Molecular docking and dynamics were performed on each ligand with the glutamate in zwitterionic form (HGlu). The orientation for each compound discussed here represents the best orientation and is representative of all possible interactions within the ligand cavity.

Taking into account that **L_4** is the ligand forming the more stable complexes, Figure 3 shows the minimum energy conformers for the adduct species [H_2**L_4**]HGlu (HpHp)(%ΔE_{C2} = −101.67 kJ mol^{-1}) and [H_3**L_4**]HGlu (HpHpHc)(%ΔE_{C2} = −126.18 kJ mol^{-1}), both of them present in 37% at pH 7.4 (Table 4). In [H_2**L_4**]HGlu, the carboxylate groups interact through hydrogen bonds with the ammonium and amine groups closer to the pyrazole moieties, as well as with the NH protons of the pyrazole rings. In [H_3**L_4**]HGlu species, in addition to the above-mentioned interactions, a $COO^-\cdots HN^+$ hydrogen bond with the central ammonium group of **L_4** is observed, together with a π-cation interaction between the ammonium glutamate group and one of the benzene rings.

NMR Studies. To gain insight into these interactions and check the speciation results with complementary techniques, we have performed a ^{1}H and ^{13}C NMR study on the interaction of the receptor **4**[**L_4**] with L-glutamate. The experiments were carried out in D_2O at pH 7.4 (pH = pD − 0.4.[38]) with a 3:1 excess of either the receptor (Table 7) or the L-glutamate (Table 8).

The ^{1}H-induced shifts experienced by L-glutamate upon interaction with **L_4** are very small (<0.1 ppm). However, the ^{13}C-induced chemical shifts ($\Delta\delta_C$) are much more significant and provide valuable information. All of the carbon atoms experience strong $\Delta\delta_C$ values which are larger for both carboxylate groups $^-$OOC-α and $^-$OOC-γ (ca. −1.2 ppm) than for the methine carbon (C-α) and methylene carbon atoms (C-β and C-γ) (ca. −1.0 ppm) (see Figure 4A).

With respect to the chemical shifts induced on the receptor by the addition of an excess of L-glutamate at pH 7.4 (Table 8), one can notice that complexation produces a general upfield shift of all the protons of **L_4** in the ^{1}H spectrum. This effect is maximum for the pyrazole ring (H-4, $\Delta\delta_H$ = −0.31 ppm), and it gradually diminishes for the aliphatic protons as the distance from the heteroaromatic ring increases [Table 8A and Figure 4B (values of $\Delta\delta$ in parentheses)]. Such a behavior suggests that the carboxylate groups should preferentially interact with the NH_2^+ groups of the receptor placed close to the pyrazole

(37) Weiner, S. J.; Kollman, P. A.; Case, D. A.; Singh, U. C.; Ghio, C.; Alagona, G.; Profeta, S., Jr.; Weiner, P. *J. Am. Chem. Soc.* **1984**, *106*, 765−784.

(38) Covington, A. K.; Paabo, M.; Robison, R. A.; Bates, R. G. *Anal. Chem.* **1968**, *40*, 700−706.

Table 6. Theoretical L-Glutamate Complexation Energies for Mono-, Di-, Tri-, and Tetraprotonated Species (ΔE_{Cn}, kJ mol^{-1}), Energetic Contribution of Each Species as a Function of Its Relative Abundance (%ΔE_{Cn}, kJ mol^{-1}), and Total Complexation Energies (ΔE_{TC}, kJ mol^{-1}) in Comparison with Experimental Association Stability Constants (K_{eff}, M^{-1})

	L_1	L_2	L_3	L_4	L_5	L_6
[HL]HGlu (%)		Hp (9)				
ΔE_{C1}		−176.86				
%ΔE_{C1}		−15.93				
[H_2L]HGlu (%)	HcHc (27)	HpHp (47)		HpHp (37)	HpHp (10)	HpHp (12)
ΔE_{C2}	−267.85	−259.33		−274.79	−208.79	−288.29
%ΔE_{C2}	−72.31	−121.89		−101.67	−20.87	−34.59
[H_3L]HGlu (%)	HpHpHc (23)	HpHpHp (7)	HpHpHp (10)	HpHpHc (37)	HpHpHp (10)	HpHpHp (12)
ΔE_{C3}	−337.91	−274.08	−279.47	−341.04	−296.07	−198.55
%ΔE_{C3}	−77.72	−19.18	−27.95	−126.18	−29.61	−23.83
[H_4L]HGlu (%)			HpHpHpHp (13)			
ΔE_{C4}			−349.49			
%ΔE_{C4}			−45.43			
ΔE_{TC}	−150.03	−157.00	−73.38	−227.85	−50.49	−58.52
K_{eff} (M^{-1})	2.44×10^3	4.12×10^3	3.99×10^2	2.04×10^4	3.51×10^2	3.64×10^2

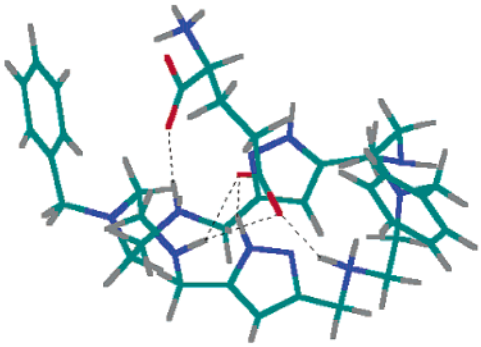

a) [H_2**L$_4$**]HGlu (Hp, Hp)
Intermolecular interactions:
(α)-COO$^-$···HN$^+$(Hp)
(γ)-COO$^-$ ···HN$^+$(Hp)
(γ)-COO$^-$···HN(Hp)
(γ)-COO$^-$···HN(Pz)

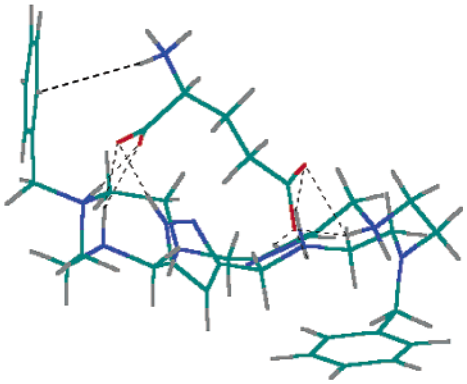

b) [H_3**L$_4$**]HGlu (Hp, Hp, Hc)
Intermolecular interactions:
(α)-COO$^-$···HN$^+$ (Hp)
(γ)-COO$^-$···HN$^+$ (Hp)
(α)-COO$^-$···HN(Pz)
(γ)-COO$^-$···HN(Pz)
(α)-COO$^-$···HN$^+$ (Hc)
$^+$NH$_3$····Ph (π interaction of T type)

Figure 3. Molecular models and interactions for L-glutamate and **L$_4$** complexes.

moiety, producing a neutralizing effect of their positive charge, because the protonation of other pyrazole-based polyaminic receptors produces a downfield shift opposite effect.[23]

Table 7. Chemical Shifts (Δδ, ppm) Induced in L-Glutamate ^{1}H and ^{13}C NMR Spectra (D_2O) at pH 7.4 by Complexation with **4**[**L$_4$**] [L:Glu (3:1)]

	G1u	L_4–Glu		Glu	L_4–Glu
H_α	3.57 dd, 1H	3.56 2dd, 1H	OOC-α	175.90	174.65
H_β	2.17 m, 2H	2.18 m, 2H	C_α	55.98	54.83
H_γ	1.90 m, 2H	1.97 m, 2H	C_β	28.28	27.11
			$C\gamma$	34.73	33.69
			OOC-γ	182.55	181.35

Table 8. Chemical Shifts (Δδ, ppm) Induced in **4**[**L$_4$**] ^{1}H and ^{13}C NMR Spectra (D_2O) at pH 7.4 by Complexation with L-Glutamate [L:Glu (1:3)]

	L_4	L_4–Glu		L_4	L_4–Glu
HC_4	6.44 s, 2H	6.13 s, 2H	$C_{3,5}$	141.58	143.81
H_2C_6	4.11 s, 8H	3.85 s, 8H	C_4	108.65	107.01
H_2C_7	3.04 t, 8H	2.86 t, 8H	C_6	44.00	44.15
H_2C_8	2.71 t, 8H	2.65 t, 8H	C_7	46.28	46.60
$H_2C_{1'}$	3.59 s, 4H	3.55 s, 4H	C_8	51.24	51.46
H_o	7.26 m, 4H	7.18 m, 4H	$C_{1'}$	58.51	59.57
H_m	7.26 m, 4H	7.18 m, 4H	C_{ipso}	137.86	138.42
H_p	7.26 m, 2H	7.18 m, 2H	C_o	131.08	131.05
			C_m	130.13	129.99
			C_p	129.31	129.17

With respect to the $\Delta\delta_C$, produced on the receptor **L$_4$** by addition of an excess of L-glutamate at pH 7.4 (Table 8, Figure 4B), in general, they are again of sign opposite to those experienced by these and related molecules when protonation occurs.[23,39] Upon protonation of the ligands, the carbon nuclei bear shielding effects that are particularly large for the atoms $C_{3,5}$ of the pyrazole ring placed in the *β*-position with respect to the nitrogen that protonates. This effect is of the same sign

(39) (a) Andrés, A.; Burguete, M. I.; García-España, E.; Luis, S. V.; Miravet, J. F.; Soriano, C. *J. Chem. Soc., Perkin Trans. 2* **1993**, *4*, 749−755. (b) Bianchi, A.; Escuder, B.; García España, E.; Luis, S. V.; Marcelino, V.; Miravet, J. F.; Ramírez, J. A. *J. Chem. Soc., Perkin Trans. 2* **1994**, *6*, 1253−1259. (c) Andrés, A.; Bazzicaluppi, C.; Bianchi, A.; García España, E.; Luis, S. V.; Miravet, J. F.; Ramírez, J. A. *J. Chem. Soc., Dalton Trans.* **1994**, *20*, 2995−3004. (d) Aguilar, J. A.; García-España, E.; Guerrero, J. A.; Llinares, J. M.; Ramírez, J. A.; Soriano, C.; Luis, S. V.; Bianchi, A.; Ferrini, L.; Fusi, V. *J. Chem. Soc., Dalton Trans.* **1996**, *2*, 239−246.

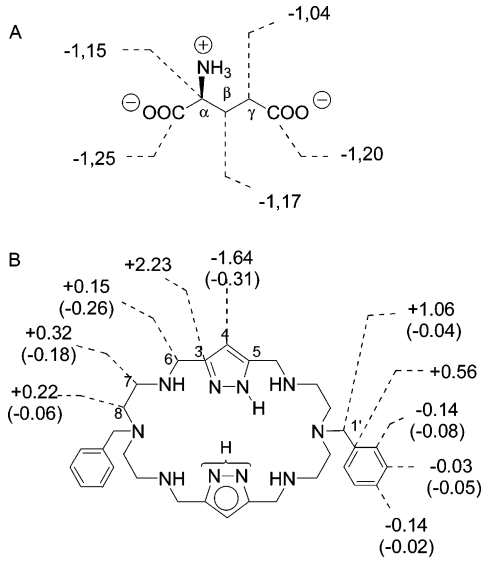

Figure 4. (A) $\Delta\delta_C$ induced upon addition of an excess of **L₄** to a L-glutamate D_2O solution at pH 7.4 [**L₄**:Glu (3:1)]. (B) $\Delta\delta_C$ and $\Delta\delta_H$ (in parentheses) induced upon addition of an excess of L-glutamate to a **L₄** D_2O solution at pH 7.4 [**L₄**:Glu (1:3)].

although of lower magnitude for the carbon atoms placed in the α-position, while for the γ-carbon C_4 is of opposite sign.

Interestingly, the interaction of **L₄** with glutamate at pH 7.4 also affects the chemical shifts of the benzyl groups, particularly those of the methylenic carbon C_1' ($\Delta\delta = 1.06$ ppm) and the quaternary carbon atom C_{ipso} ($\Delta\delta = 0.56$ ppm). The aromatic carbon atoms C_o and C_p also experience some shift (−0.14 ppm). All of these facts suggest that the interaction of L-glutamate with **L₄** brings about significant conformational changes of the benzylic groups and that in addition to the secondary amino groups closer to the pyrazole rings, the central tertiary *N*-Bn substituted amino groups are also participating in the interaction with L-glutamate.[12]

Finally, we have measured NOE effects (from ROESY and NOESY NMR spectra) of **L₄** in the presence of an excess of L-glutamate in H_2O/D_2O at pH 7.4. The spectra did not show evidence of intermolecular cross-peaks. The only NOE effects observed were intramolecular cross-peaks. Taking into account that molecular modeling studies indicate that the closest distances between the protons of L-glutamate and those of **L₄** are above 4 Å in both conformers (Figure 3a and 3b) and that beyond the 3.0 Å range the NOE is very weak, these results indicate that in agreement with the theoretical geometries it is not possible to detect intermolecular distances in the **L₄**−L-glutamate complex.

Conclusions

Hexaaza 2+2 dipodal macrocycles containing 1*H*-pyrazole rings as spacers show a good ability for interacting with L-glutamic acid in water. Controlled structural modifications introduced in the receptors allow for the derivation of the following general considerations regarding the structure−interaction strength relationship: (i) the central nitrogens of the chain are implicated in the interaction with pyrazole as shown by the decrease in stability observed when exchanging these nitrogens by carbon atoms; (ii) the receptors with secondary nitrogens in the middle of the side chains show a reverse dependence of the effective constants with pH; and (iii) the functionalization of the central nitrogens of the side chains with benzyl groups (**L₄**) yields a sharp increase in stability ($K_{eff} = 2.0 \times 10^4$ at pH 7.4), while the introduction of phenethyl groups originates the opposite effect ($K_{eff} = 3.51 \times 10^2$ at pH 7.4). Molecular modeling and NMR analysis suggest that in addition to $COO^-\cdots{}^+H_2N$, $COO^-\cdots{}^+HNBn$, $COO^-\cdots HN$, and $COO^-\cdots HPz$ hydrogen bonds, π-cation interactions may be contributing to the extra stabilization of the glutamic adducts with **L₄**. In the case of this receptor, we have also studied its association constants with L-aspartate. The data show a 15-fold selectivity of L-glutamate over L-aspartate at pH 7.4.

Experimental Section

The starting materials were purchased from commercial sources and used without further purification. The solvents were dried using standard techniques. All reactions were monitored by thin-layer chromatography using DC-Alufolien silica gel $60PF_{254}$ (Merck; layer thickness, 0.2 mm). Compounds were detected UV light (254 nm), with iodine, or with phosphomolybdic acid reagent. Melting points were determined in a Reichert-Jung hot-stage microscope and are uncorrected. ^1H and ^{13}C NMR spectra were recorded on Varian Inova-300, Varian Inova-400, and Varian Unity-41500 spectrometers. The chemical shifts are reported in ppm using dioxane ($\delta = 67.4$ ppm) as an internal reference in D_2O. All assignments have been performed on the basis of $^1H-^{13}C$ heteronuclear multiple quantum coherence experiments (gHSQC and gHMBC). In the NMR study of the complexation of ligands with glutamic acid in D_2O, the pH was calculated from the measured pD values using the correlation pH = pD − 0.4. IR spectra were recorded with a Perkin-Elmer Spectrum One spectrophotometer. The mass spectra (MS) were registered in a Hewlett-Packard 1100 MSD spectrometer by electrospray positive mode (ES^+). Elemental analyses were provided by the Departamento de Análisis, Centro de Química Orgánica "Manuel Lora Tamayo", CSIC, Madrid, Spain.

Preparation of the 3,5-Pyrazoledicarbaldehyde (7a). It was prepared from 3,5-bis(hydroximethyl)pyrazole by oxidation with MnO_2 in DME as previously reported.[23]

Preparation of Precursor Amines. 1,5-Diphthalimido-3-azapentane (9). A mixture of 1,5-diamino-3-azapentane (10.3 g, 0.10 mol) and phthalic anhydride (33.2 g, 0.20 mol) in 160 mL of glacial acetic acid was refluxed for 4 h. The solvent was removed under reduced pressure, and then 160 mL of hot ethanol was added with stirring until a solid appeared. The product was collected and washed with cold ethanol. Yield 23.9 g (81%), mp 181−183 °C, lit.[24a] 182−183 °C. ^1H NMR (DMSO-d_6, 300 MHz): 7.79 (m, 4H, $H_{3',6'}$), 7.74 (m, 4H, $H_{4',5'}$), 3.59 (t, $J = 6.3$ Hz, 4H, $H_{1,5}$), 2.76 (t, 4H, $H_{2,4}$). ^{13}C NMR (75 MHz, DMSO-d_6): 167.85 (CO), 134.10 ($C_{4',5'}$), 131.63 ($C_{1',2'}$), 122.74 ($C_{3',6'}$), 46.16 ($C_{2,4}$), 37.18 ($C_{1,5}$). MS (ES^+, MeOH): *m*/*z* 364 (MH^+). Anal. Calcd (%) for $C_{20}H_{17}N_3O_4$ (363.37): C, 66.11; H, 4.72; N, 11.56. Found: C, 66.30; H, 4.80; N, 11.88.

General Procedure for Alkylation. A solution of **9** (7.260 g, 20 mmol) and a variable amount of benzyl, phenethyl, or octyl bromide in 300 mL of MeCN was refluxed with stirring in the presence of K_2CO_3. The solvent was removed on a rotatory evaporator, and the dry residue was treated with H_2O (100 mL) and extracted with dichloromethane (3 × 50 mL). This extract was dried with anhydrous $MgSO_4$ and evaporated to give a solid, which was purified by flash column chromatography on silicagel (hexane−EtOAc, 95:5 to 40:60).

3-Benzyl-1,5-diphthalimido-3-azapentane (10a). This was prepared by reaction of **9**, benzyl bromide (4.27 g, 25 mmol), and potassium carbonate (3.45 g, 25 mmol) for 12 h to give a white solid. Yield 8.23 g (91%), mp 130−131 °C, lit.[24b] 130−132 °C. ^1H NMR (400 MHz, $CDCl_3$): 7.71 (m, 4H, $H_{3',6'}$), 7.67 (m, 4H, $H_{4',5'}$), 7.05 (d, $J = 7.2$ Hz, 2H, H_o), 7.02 (t, $J = 7.3$ Hz,1H, H_p), 6.92 (d, 2H, H_m), 3.76 (t, $J = 6.3$ Hz, 4H, $H_{1,5}$), 3.66 (s, 2H, $H_{1''}$), 2.80 (t, 4H, $H_{2,4}$). ^{13}C NMR (100 MHz, $CDCl_3$): 168.08 (CO), 138.67 (C_{ipso}), 133.52 ($C_{4',5'}$), 132.33 ($C_{1',2'}$), 128.86 (C_o), 127.94 (C_m), 126.73 (C_p), 122.94 ($C_{3',6'}$), 58.16 ($C_{1''}$), 51.62

($C_{2,4}$), 35.70 ($C_{1,5}$). MS (ES^+, MeCN/MeOH): *m/z* 454 (MH^+). Anal. Calcd (%) for $C_{27}H_{23}N_3O_4$ (453.59): C, 71.51; H, 5.11; N, 9.27. Found: C, 71.80; H, 5.43; N, 9.52.

3-Phenethyl-1,5-diphthalimido-3-azapentane (10b). This was prepared by reaction of **9**, phenethyl bromide (11.10 g, 60 mmol), and potassium carbonate (8.28 g, 60 mmol) for 4 days to give a white solid. Yield 4.48 g (48%). ^1H NMR (400 MHz, $CDCl_3$): 7.74 (m, 4H, $H_{3',6'}$), 7.67 (m, 4H, $H_{4',5'}$), 7.18 (m, 2H, H_m), 7.15 (m, 2H, H_o), 7.08 (m, 1H, H_p), 3.74 (t, $J = 6.6$ Hz, 4H, $H_{1,5}$), 2.86 (t, 4H, $H_{2,4}$), 2.81 (s, 2H, $H_{1''}$), 2.62 (s, 2H, $H_{2''}$). ^{13}C NMR (100 MHz, $CDCl_3$): 168.24 (CO), 140.07 (C_{ipso}), 133.69 ($C_{4',5'}$), 132.23 ($C_{1',2'}$), 128.75 (C_m), 128.20 (C_o), 125.81 (C_p), 123.08 ($C_{3',6'}$), 55.64 ($C_{1''}$), 51.58 ($C_{2,4}$), 35.81 ($C_{1,5}$), 33.78 ($C_{2''}$). IR (KBr, cm^{-1}): 1771, 1701. MS (ES^+, MeCN/MeOH): *m/z* 468 (MH^+). Anal. Calcd (%) for $C_{28}H_{25}N_3O_4$ (467.52): C, 71.93; H, 5.39; N, 8.99. Found: C, 72.21; H, 5.60; N, 9.04.

3-Octyl-1,5-diphthalimido-3-azapentane (10c). This was prepared by reaction of **9**, octyl bromide (11.58 g, 60 mmol), and potassium carbonate (8.28 g, 60 mmol) for 4 days to give a yellow oil. Yield 8.26 g (87%). ^1H NMR (400 MHz, $CDCl_3$): 7.75 (m, 4H, $H_{3',6'}$), 7.68 (m, 4H, $H_{4',5'}$), 3.73 (t, $J = 6.7$ Hz, 4H, $H_{1,5}$), 2.78 (t, 4H, $H_{2,4}$), 2.50 (t, $J = 7.1$ Hz, 2H, $H_{1''}$), 1.15 (m, 12H, $H_{2''}$, $H_{3''}$, $H_{4''}$, $H_{5''}$, $H_{6''}$, $H_{7''}$), 0.84 (t, $J = 7.1$ Hz, 3H, $H_{8''}$). ^{13}C NMR (100 MHz, $CDCl_3$): 168.25 (CO), 133.66 ($C_{4',5'}$), 132.17 ($C_{1',2'}$), 123.01 ($C_{3',6'}$), 53.92 ($C_{1''}$), 51.49 ($C_{2,4}$), 35.84 ($C_{1,5}$), 31.75 ($C_{6''}$), 29.51, 29.21, 27.22 ($C_{2''}$, $C_{3''}$, $C_{4''}$, $C_{5''}$), 22.59 ($C_{7''}$), 14.08 ($C_{8''}$). IR (KBr, cm^{-1}): 1755, 1695. MS (ES^+, MeCN/MeOH): *m/z* 476 (MH^+). Anal. Calcd (%) for $C_{28}H_{33}N_3O_4$ (475.58): C, 70.71; H, 6.99; N, 8.84. Found: C, 70.89; H, 7.21; N, 8.91.

General Procedure of Deprotection. Working under argon atmosphere, a solution of **10a**, **10b**, or **10c** (12 mmol) and hydrazine monohydrate (12.0 g, 240 mmol) in 500 mL of EtOH was refluxed with vigorous stirring for 36 h. The mixture was filtered and washed with EtOH. The solvent was removed, and then 300 mL of $CHCl_3$ was added, and after the mixture was stirred overnight, the insoluble phthalhydrazide was filtered off. Evaporation of $CHCl_3$ gave a yellow oil which was purified by distillation under reduced pressure to give the corresponding diamine.

1,5-Diamino-3-benzyl-3-azapentane (11a). Colorless oil. Yield 1.48 g (63%), bp 51−54 °C (0.1 mmHg). ^1H NMR (300 MHz, $CDCl_3$): 7.26 (m, 5H, H_o, H_m, H_p), 3.57 (s, 2H, $H_{1'}$), 2.74 (t, $J = 6.0$ Hz, 4H, $H_{1,5}$), 2.50 (t, 4H, $H_{2,4}$), 1.29 (bs, 4H, NH). ^{13}C NMR (75 MHz, $CDCl_3$): 139.44 (C_{ipso}), 128.65 (C_o), 128.11 (C_m), 126.81 (C_p), 59.01 ($C_{1'}$), 57.20 ($C_{2,4}$), 39.63 ($C_{1,5}$). IR (KBr, cm^{-1}): 3350−3100. MS (ES^+, MeOH): *m/z* 194 (MH^+). Anal. Calcd (%) for $C_{11}H_{19}N_3$ (193.29): C, 68.35; H, 9.91; N, 21.74. Found: C, 67.98; H, 10.21; N, 22.04.

1,5-Diamino-3-phenethyl-3-azapentane (11b). Colorless oil. Yield 1.42 g (57%), bp 89−94 °C (0.5 mmHg). ^1H NMR (300 MHz, $CDCl_3$): 7.24 (m, 2H, H_m), 7.14 (m, 3H, H_o, H_p), 2.81 (m, 2H, $H_{1'}$), 2.66 (t, $J = 5.9$ Hz, 4H, $H_{1,5}$), 2.62 (m, 2H, $H_{2'}$), 2.49 (t, 4H, $H_{2,4}$), 1.42 (bs, 4H, NH). ^{13}C NMR (75 MHz, $CDCl_3$): 140.49 (C_{ipso}), 128.58 (C_o), 128.18 (C_m), 125.81 (C_p), 56.96 ($C_{2,4}$), 55.98 ($C_{1'}$), 39.64 ($C_{1,5}$), 33.56 ($C_{2'}$). IR (KBr, cm^{-1}): 3400−3200. MS (ES^+, MeOH): *m/z* 208 (MH^+).

1,5-Diamino-3-*n*-octyl-3-azapentane (11c). Colorless oil. Yield 1.39 g (54%), bp 66−68 °C (0.1 mmHg). ^1H NMR (300 MHz, $CDCl_3$): 2.71 (t, $J = 6.0$ Hz, 4H, $H_{1,5}$), 2.45 (t, 4H, $H_{2,4}$), 2.38 (m, 2H, $H_{1'}$), 1.32 (m, 12H, $H_{2'}$, $H_{3'}$, $H_{4'}$, $H_{5'}$, $H_{6'}$, $H_{7'}$), 0.85 (t, $J = 6.4$ Hz, 3H, $H_{8'}$). ^{13}C NMR (75 MHz, $CDCl_3$): 57.26 ($C_{2,4}$), 54.51 ($C_{1'}$), 39.56 ($C_{1,5}$), 31.84 ($C_{6'}$), 29.55, 29.32, 27.49, 27.19 ($C_{2'}$, $C_{3'}$, $C_{4'}$, $C_{5'}$), 22.64 ($C_{7'}$), 14.09 ($C_{8'}$). IR (KBr, cm^{-1}): 3400−3100. MS (ES^+, MeOH): *m/z* 216 (MH^+). Anal. Calcd (%) for $C_{12}H_{29}N_3$ (215.38): C, 66.92; H, 13.57; N, 19.51. Found: C, 66.67; H, 13.85; N, 19.70.

Preparation of Macrocyclic Ligands. Ligands **1** and **2** were prepared by reaction of the 3,5-pyrazoledicarbaldehyde 1*H*- or 1-benzyl substituted, respectively, with 1,5-diamino-3-azapentane as previously reported.[23]

3,9,12,13,16,22,25,26-Octaazatricyclo-[22.2.1.1^{11,14}]-octacosa-1(27),2,9,11,14(28),15,22,24-octaene (8). Working under an argon atmosphere, a solution of 3,5-pyrazoledicarbaldehyde (496 mg, 4 mmol) in methanol (200 mL) was added dropwise to a stirred solution of 1,5-pentanediamine (448 mg, 4.4 mmol) in methanol (120 mL). After the mixture was stirred for 12 h, a white solid was formed, and then it was filtered off, successively washed with methanol and Et_2O, and dried in vacuo. Yield 529 mg (68%), mp 208−210 °C. ^1H NMR (300 MHz, DMSO-d_6): δ 8.13 (s, 4H, H_6), 6.58 (s, 2H, H_4), 3.52 (m, 8H, H_7), 1.60 (m, 8H, H_8), 1.07 (m, 4H, H_9). IR (KBr, cm^{-1}): 1645. MS (ES^+, MeOH): *m/z* 381 (MH^+). Anal. Calcd (%) for $C_{20}H_{36}N_8 \cdot 0.5H_2O$ (389.50): C, 61.67; H, 7.50; N, 28.77. Found: C, 61.91; H, 7.81; N, 28.34.

3,9,12,13,16,22,25,26-Octaazatricyclo-[22.2.1.1^{11,14}]-octacosa-1(27),-11,14(28),24-tetraene (3). To a stirred suspension of the Schiff base **8** (389 mg, 1 mmol) in methanol (150 mL) was added sodium borohydride (456 mg, 12 mmol) portionwise. The mixture was stirred for 2 h, the solvent was then removed, and the dry residue was purified by extracting with toluene in a Soxhlet apparatus to give a solid which was recrystallized from toluene. Yield 432 mg (54%), mp (toluene) 184−186 °C. ^1H NMR (300 MHz, $CDCl_3$): δ 6.00 (s, 2H, H_4), 3.79 (s, 8H, H_6), 2.62 (t, *J* 5.8 Hz, 8H, H_7), 1.48 (m, 8H, H_8), 1.48 (m, 4H, H_9). ^{13}C NMR (75 MHz, $CDCl_3$): 147.01 (broad singlet, $C_{3,5}$), 102.51 (C_4), 48.23 (C_7), 45.68 (C_6), 28.51 (C_8), 23.85 (C_9). IR (KBr, cm^{-1}): 3380. MS (ES^+, MeOH): *m/z* 389 (MH^+). Anal. Calcd (%) for $C_{20}H_{36}N_8$ (388.55): C, 61.82; H, 9.34; N, 28.84. Found: C, 61.70; H, 9.48; N, 28.59.

6,19-Dibenzyl-3,6,9,12,13,16,19,22,25,26-decaazatricyclo-[22.2.1.1^{11,14}]-octacosa-1(27),11,14(28),24-tetraene (4). 3,5-Pyrazoledicarbaldehyde (248 mg, 2 mmol) was dissolved in hot methanol (120 mL). This solution was then cooled to room temperature and added dropwise under an argon atmosphere to a stirred solution of the diamine **11a** (387 mg, 2 mmol) in methanol (200 mL). The reaction was monitored by TLC (Cl_3CH/MeOH 10:1), and when it was complete (ca. 12 h), sodium borohydride (456 mg, 24 mmol) was added portionwise. After 2 h of reaction, the solvent was evaporated to dryness under reduced pressure. The residual syrup was purified by flash column chromatography on silica gel (MeOH/30% aqueous NH_3 48:2). The fractions containing the product of R_f 0.37 (TLC, MeOH/ 30% aqueous NH_3 10:1) were evaporated to dryness to give a pure colorless syrup. Yield 295 mg (51%). ^1H NMR ($CDCl_3$, 400 MHz): 7.29 (m, 4H, H_o), 7.24 (m, 4H, H_m), 7.18 (m, 2H, H_p), 5.94 (s, 2H, H_4), 3.75 (s, 8H, H_6), 3.61 (s, 4H, $H_{1'}$), 2.80 (t, $J = 5.3$ Hz, 8H, H_7), 2.69 (t, 8H, H_8). ^{13}C NMR (100 MHz, $CDCl_3$): 146.21 (very broad signal, $C_{3,5}$), 138.92 (C_{ipso}), 128.74 (C_o), 128.26 (C_m), 126.93 (C_p), 101.09 (broad singlet, C_4), 59.00 ($C_{1'}$), 53.05 (broad singlet, C_8), 46.98 (C_7), 46.25 (broad singlet, C_6). IR (KBr, cm^{-1}): 3435. MS (ES^+, MeOH): *m/z* 572 (MH^+). Anal. Calcd (%) for $C_{32}H_{46}N_{10} \cdot 0.25OHNH_4$ (578.75): C, 66.34; H, 8.16; N, 24.79. Found: C, 66.22; H, 8.40; N, 24.82.

6,19-Diphenethyl-3,6,9,12,13,16,19,22,25,26-decaazatricyclo-[22.2.1.1^{11,14}]-octacosa-1(27),11,14(28),24-tetraene (5). This compound was prepared as described for **4** from the diamine **11b** (414 mg) to give a colorless syrup of R_f 0.56 (TLC, MeOH/30% aqueous NH_4OH 10:1). Yield 380 mg (63%). ^1H NMR ($CDCl_3$, 400 MHz): 7.06 (d, $J = 7.2$ Hz, 4H, H_o), 6.98 (t, 4H, H_m), 6.81 (t, 2H, H_p), 5.91 (s, 2H, H_4), 3.64 (s, 8H, H_6), 2.68 (m, 8H, H_7), 2.63 (m, 8H, H_8, $H_{1'}$, $H_{2'}$). ^{13}C NMR (100 MHz, $CDCl_3$): 145.73 (very broad signal, $C_{3,5}$), 140.81 (C_{ipso}), 128.63 (C_o), 128.01 (C_m), 125.72 (C_p), 100.91 (broad singlet, C_4), 55.06 (very broad singlet, $C_{1'}$), 52.13 (broad singlet, C_8), 46.71 (C_7), 46.42 (broad singlet, C_6), 33.11 ($C_{2'}$). IR (KBr, cm^{-1}): 3430. MS (ES^+, MeOH): *m/z* 600 (MH^+). Anal. Calcd (%) for $C_{34}H_{50}N_{10} \cdot 1.5H_2O$ (625.0): C, 65.28; H, 8.48; N, 22.40. Found: C, 65.55; H, 8.33; N, 22.56.

6,19-Dioctyl-3,6,9,12,13,16,19,22,25,26-decaazatricyclo-[22.2.1.1^{11,14}]-octacosa-1(27),11,14(28),24-tetraene (6). This compound was prepared as described for **4** from the diamine **11c** (430 mg) to give a colorless

syrup of R_f 0.54 (TLC, MeOH/30% aqueous NH_4OH 10:1). Yield 204 mg (31%). ^{1}H NMR ($CDCl_3$, 400 MHz): 6.11 (s, 2H, H_4), 3.81 (s, 8H, H_6), 2.84 (m, 8H, H_7), 2.65 (m, 8H, H_8), 2.48 (m, 4H, $H_{1'}$), 1.41 (m, 4H, $H_{2'}$), 1.21 (m, 20H, $H_{3'}$, $H_{4'}$, $H_{5'}$, $H_{6'}$, $H_{7'}$), 0.83 (t, $J = 6.7$ Hz, 6H, $H_{8'}$). ^{13}C NMR (100 MHz, $CDCl_3$): 145.67 (very broad signal, $C_{3,5}$), 102.47 (broad singlet, C_4), 54.18 (broad singlet, $C_{1'}$), 51.29 (broad singlet, C_8), 46.98 (C_7), 45.30 (broad singlet, C_6), 31.79 ($C_{6'}$), 29.49, 29.25, 27.51, 25.88 ($C_{2'}$, $C_{3'}$, $C_{4'}$, $C_{5'}$), 22.6 ($C_{7'}$), 14.1 ($C_{8'}$). IR (KBr, cm^{-1}): 3422. MS (ES$^+$, MeOH): *m*/*z* 616 (MH^+). Anal. Calcd (%) for $C_{34}H_{66}N_{10}\cdot 2H_2O$ (833.72): C, 62.73; H, 10.84; N, 21.52. Found: C, 63.07; H, 10.95; N, 21.78.

General Procedure for Preparation of the Hydrochlorides. Ligands **3**, **4**, **5**, and **6** descompose partially after some time, and it is preferable to store them as the corresponding hydrochlorides, prepared as follows: A mixture of the corresponding ligand (0.5 mmol) and 1 M aqueous hydrochloric acid (3 mL) was stirred for 12 h. After addition of ethanol (50 mL), the solvent was evaporated to dryness. Next, 30 mL of ethanol was added, and the resulting solution was stirred for 1 h. A white solid was formed, filtered off, and dried over phosphorus pentoxide at 60 °C for 48 h.

[3]·4HCl. Yield 219 mg (82%), mp 225−227 °C. ^{1}H NMR (D_2O, 300 MHz): δ 6.68 (s, 2 H, H_4), 4.35 (s, 8 H, H_6), 2.96 (t, $J = 6.3$ Hz, 8 H, H_7), 1.63 (m, 8 H, H_8), 1.37 (m, 4 H, H_9). ^{13}C NMR (D_2O, 75 MHz): 139.00 ($C_{3,5}$), 108.55 (C_4), 45.99 (C_7), 41.99 (C_6), 24.83 (C_8), 22.84 (C_9). IR (KBr, cm^{-1}): 3395. MS (ES$^+$, H_2O): *m*/*z* 389 ([MH − 4HCl]$^+$). Anal. Calcd (%) for $C_{20}H_{36}N_8\cdot 4HCl$ (534.40): C, 44.95; H, 7.54; N, 20.97. Found: C, 44.61; H, 7.17; N, 20.82.

[4]·6HCl. Yield 210 mg (52%), mp 238−240 °C. ^{1}H NMR (D_2O, 300 MHz): δ 7.35 (s, 10 H, H_o, H_m, H_p), 6.58 (s, 2 H, H_4), 4.16 (s, 8 H, H_6), 3.89 (s, 4 H, $H_{1'}$), 3.22 (t, $J = 6.3$ Hz, 8 H, H_7), 3.01 (t, 8 H, H_8). ^{13}C NMR (D_2O, 75 MHz): 139.95 ($C_{3,5}$), 132.53 (C_{ipso}), 131.86, 130.64 (C_o, C_m), 131.00 (C_p), 109.91 (C_4), 59.64 ($C_{1'}$), 50.51 (C_8), 43.87 (C_6), 43.59 (C_7). IR (KBr, cm^{-1}): 3440. MS (ES$^+$, H_2O): *m*/*z* 572 ([MH − 6HCl − H_2O]$^+$). Anal. Calcd (%) for $C_{32}H_{46}N_{10}\cdot 6HCl\cdot H_2O$ (807.55): C, 47.59; H, 6.74; N, 17.34. Found: C, 47.24; H, 7.11; N, 16.84.

[5]·6HCl. Yield 318 mg (78%), mp 221−223 °C. ^{1}H NMR (D_2O, 500 MHz): δ 7.24 (t, 4 H, H_o, H_m), 7.17 (m, 6 H, H_p), 6.58 (s, 2 H, H_4), 4.16 (s, 8 H, H_6), 3.89 (s, 4 H, $H_{1'}$), 3.22 (t, $J = 6.3$ Hz, 8 H, H_7), 3.01 (t, 8 H, H_8). ^{13}C NMR (D_2O, 125 MHz): 139.79 ($C_{3,5}$), 137.41 (C_{ipso}), 130.30 (C_m), 130.01 (C_o), 128.58 (C_p), 110.10 (C_4), 55.98 ($C_{1'}$), 50.00 (C_8), 43.87 (C_6), 42.44 (C_7), 30.54 ($C_{2'}$). IR (KBr, cm^{-1}): 3435. MS (ES$^+$, H_2O): *m*/*z* 600 ([MH − 6HCl]$^+$). Anal. Calcd (%) for $C_{34}H_{50}N_{10}\cdot 6HCl$ (817.59): C, 49.95; H, 6.90; N, 17.13. Found: C, 50.16; H, 7.00; N, 17.18.

[6]·6HCl. Yield 312 mg (75%), mp 228−231 °C. ^{1}H NMR (D_2O, 400 MHz): 6.57 (s, 2H, H_4), 4.22 (s, 8H, H_6), 3.36 (m, 8H, H_8), 3.30 (m, 8H, H_7), 3.04 (t, $J = 8.0$ Hz, 4H, $H_{1'}$), 3.22 (m, 4H, $H_{2'}$), 1.06 (m, 10H, $H_{3'}$, $H_{4'}$, $H_{5'}$, $H_{6'}$, $H_{7'}$), 0.61 (t, $J = 6.6$ Hz, 6H, $H_{8'}$). ^{13}C NMR (D_2O, 100 MHz): 139.68 ($C_{3,5}$), 110.18 (C_4), 55.52 ($C_{1'}$), 49.87 (C_8), 43.89 (C_6), 41.81 (C_7), 32.11 ($C_{6'}$), 29.33 ($C_{4'}$, $C_{5'}$), 26.73 ($C_{3'}$), 23.97 ($C_{2'}$), 23.13 ($C_{7'}$), 14.55 ($C_{8'}$). IR (KBr, cm^{-1}): 3434. MS (ES$^+$, H_2O): *m*/*z* 616 ([MH − 6HCl]$^+$). Anal. Calcd (%) for $C_{34}H_{66}N_{10}\cdot 6HCl$ (833.72): C, 48.98; H, 8.70; N, 16.80. Found: C, 48.69; H, 8.76; N, 16.72.

Electromotive Force (emf) Measurements. The potentiometric titrations were carried out in 0.15 M NaCl at 298.1 ± 0.1 K by using the experimental procedure (buret, potentiometer, cell, stirrer, microcomputer, etc.) that has been fully described elsewhere.[40] The acquisition of the emf data was performed with the computer program PASAT.[41] The reference electrode was a Ag/AgCl electrode in saturated KCl solution. The glass electrode was calibrated as a hydrogen ion concentration probe by titration of well-known amounts of HCl with CO_2-free NaOH solutions and determination of the equivalent point by Gran's method,[42] which gives the standard potential $E^{\circ\prime}$ and the ionic product of water [pK_w = 13.73(1)]. The computer program HYPERQUAD[43] was used to calculate the protonation and stability constants, and the HYSS[44] program was used to obtain the distribution diagrams. The titration curves for each system (ca. 200 experimental points corresponding to at least three measurements, pH 2−11, concentration of ligands 1×10^{-3} to 5×10^{-3} M) were treated either as a single set or as separated curves without significant variations in the values of the stability constants. Finally, the sets of data were merged together and treated simultaneously to give the final stability constants.

Molecular Modeling. L-Glutamic acid was modeled as zwitterion, as this was the principal structure in the pH range of experimental studies, and ligands were modeled in all posible protonation states showed to exist in the pH range of experimental data in 5% or more abundance. Starting structures for ligands were built by using Hyperchem capabilities. Its geometry was minimized to a maximum energy gradient of 0.4 kJ/(A mol) with the AMBER force field, using the Polak-Ribiere (conjugate gradient) algorithm, and the "simulated annealing" procedure was used to cover all conformational space runnning molecular dynamics at 400 K. This geometry was always used in all calculations of host/guest complexes. To optimize host/guest interactions, the L-glutamic acid was moved and/or rotated around the C_2-C_3 bond and the structure of the acid was docked into the "cavity" of the ligand in all different possible orientations, and then the energy of the complex was minimized with no restraints, following the same procedure as above.

Acknowledgment. This work is devoted to the memory of Prof. Manuel Lora-Tamayo. Financial support by the Spanish "Comisión Interministerial de Ciencia y Tecnología" (CICYT, Proyects SAF-99-0063, and BQU2003-09215-CO3-01) is gratefully acknowledged.

Supporting Information Available: Potentiometric data: Figure S_1 (distribution diagrams for the systems $\mathbf{L_n}-H^+$ and Glu$-H^+$) and Figure S_2 (distribution diagrams for the systems $\mathbf{L_2}-$glutamic acid, $\mathbf{L_3}-$glutamic acid, and $\mathbf{L_6}-$glutamic acid). Molecular modelization data: Figures S_3 and S_4 (charges and AMBER atom type for 3,5-bis[(*N*-methylamino)methyl]-1*H*-pyrazol and for 1-benzyl-3,5-bis[(*N*-methylamino)-methyl]-pyrazol), Table S_1 (nonstandard force field parameters used in this work), Table S_2 (energy variations for ligands $\mathbf{L_1}-\mathbf{L_6}$ with protonation pattern), Tables S_3-S_8 (calculation of complexation energy for $\mathbf{L_1}-\mathbf{L_6}$), Table S_9 (stability constants for the system Asp$-\mathbf{L_4}$), Figure S_5 (representation of the variation of K_{cond} (M^{-1}) for the interaction of glutamic and aspartic acids with $\mathbf{L_4}$; initial concentrations of acids and receptors are 10^{-3} M), and Figures S_6-S_{10} (molecular models and interactions for the L-glutamate adducts formed from ligands $\mathbf{L_1}-\mathbf{L_3}$ and $\mathbf{L_5}$,$\mathbf{L_6}$) (PDF). This material is available free of charge via the Internet at http://pubs.acs.org.

JA035671M

(40) García-España, E.; Ballester, M. J.; Lloret, F.; Moratal, J.-M.; Faus, J.; Bianchi, A. *J. Chem. Soc., Dalton Trans.* **1988**, *2*, 101−104.

(41) Fontanelli, M.; Micheloni, M. *Proceedings of the 1st Spanish-Italian Congress on Thermodynamics of Metal Complexes*; Diputación de Castellón: Peñíscola (Castellón), España, 3−6 Junio 1990.

(42) (a) Gran, G. *Analyst (London)* **1952**, *77*, 661. (b) Rossoti, F. J. C.; Rossoti, H. *J. Chem. Educ.* **1965**, *42*, 375−378.

(43) Gans, P.; Sabatini, A.; Vacca, A. *Talanta* **1996**, *43*, 1739−1753.

(44) Gans, P. Program to determine the distribution of species in multiequilibria systems from the stability constants and mass balance equations.